CDF note 7155

Search for the Quasi-Stable Doubly-Charged Higgs Using the Two-Track Signature

The CDF Collaboration
URL http://www-cdf.fnal.gov
(Dated: July 31, 2004)

We describe our search for a long-lived doubly-charged Higgs particle in CDF Run II. We anticipate a signature of two highly ionizing tracks with penetration in the detector similar to that of a muon. Our search uses 206 pb^{-1} of high P_T muon data collected between February, 2002 and September, 2003. Having found no candidate event in the two-track search region, we set a mass limit of 134 GeV on quasi-stable $H^{\pm\pm}$ production.

Preliminary Results for Summer 2004 Conferences

I. INTRODUCTION

This note describes a search for quasi-stable doubly-charged Higgs in $\bar{p}p$ collisions at $\sqrt{s} = 1.96$ TeV with the CDFII detector at the Fermilab Tevatron. The CDFII detector is described in detail in [1].

The introduction of a Higgs triplet containing neutral, singly, and doubly-charged members is required in the Left-Right Symmetric Model. Due to spontaneous symmetry breaking in this model, if there is supersymmetry and if the doubly-charged Higgs is part of the right-handed triplet resulting in low left-handed neutrino masses, then the supersymmetric terms are suppressed by the Planck scale. This motivates a relatively lightweight Higgs within reach of the Tevatron, having its mass determined solely by the right-handed mass scale and the Planck mass.

Other CDFII searches have focused on dilepton decays of the doubly-charged Higgs. No evidence for doubly-charged Higgs production was observed in these searches, but lower mass limits were set in the ee, $e\mu$, and $\mu\mu$ channels at 133 GeV/c^2, 136 GeV/c^2, and 115 GeV/c^2 respectively for $H_L^{\pm\pm}$ and 113 GeV/c^2 in the $\mu\mu$ channel for $H_R^{\pm\pm}$ [2].

In this search, we consider the case of no intra-detector decay ($c\tau > 3$m) of the doubly-charged particle. The existing mass limit for long-lived $H^{\pm\pm}$ was set at LEP2 by the DELPHI collaboration at 97.3 GeV/c^2 [3]. We made the decision to divide our search *a priori* into a "loose" search (for setting limits) and a "tight" search (for claiming discovery), which are both described here.

Massive charged particles traveling post-collision through the CDF detector primarily lose energy due to ionization. Ionization produced by these particles is given by the Bethe-Bloch equation [4]:

$$-\frac{dE}{dx} = Kz^2\frac{Z}{A}\frac{1}{\beta^2}[\frac{1}{2}\ln(\frac{2m_ec^2\beta^2\gamma^2T_{max}}{I^2}) - \beta^2 - \frac{\delta}{2}], \quad (1)$$

where z is the charge of the incident particle.

Since the ionization of a particle is proportional to the square of its charge, a doubly-charged particle would cause four times the ionization of a singly-charged one. We exploit this large difference in ionization in our search for a long-lived doubly-charged Higgs.

II. DATA SAMPLE & EVENT SELECTION

This analysis is based on an integrated luminosity of 206 pb^{-1} collected with the CDFII detector between February 2002 and September 2003. The data are collected with an inclusive muon trigger that requires at least one muon with P_T >18 GeV/c. From this inclusive dataset we select events offline having both a reconstructed isolated muon and second track whose P_T are each greater than 20 GeV. The P_T is reconstructed under the assumption that the particle carries only unit charge. Both muon and track are required to be "highly ionizing," a quality we define below. We also reject events having cosmics identified by a cosmic ray tagger.

A. Ionization Cuts

Energy loss due to ionization can be measured several different ways within the CDF detector. We employ the combined dE/dx measurements of calorimeters and tracking devices to get a complete picture of a particle's ionization.

Both the hadronic and electromagnetic calorimeters measure dE/dx for minimum-ionizing particles. We use these energy-depositions as recorded by each calorimeter along the track of the particle whose ionization we want to measure. We call these quantities E_{Had} and E_{EM} respectively.

The Central Outer Tracking chamber (COT) also encodes dE/dx information in the width of the pulse of each hit, and provides a particularly useful ionization measurement. In this analysis we use these calibrated COT dE/dx measurements.

We define two separate sets of ionization cuts in our analysis. The loose cuts seek to maximize efficiency and are used exclusively for setting a mass limit. The tight cuts on the other hand are used to virtually eliminate the fake backgrounds and will be used only in case of discovery. Since the combined cuts on E_{EM} and E_{Had} are found to be fairly inefficient, the ability to set a limit suffers when using them. Thus, we completely removed these calorimeter cuts in the loose search category. We optimized the ionization cuts and settled on tight cut values of $E_{EM} > 0.6$ GeV, $E_{Had} > 4$ GeV, and COT $dE/dx > 35$ ns. In order for a particle to fulfill the loose requirements, it must pass only the COT $dE/dx > 35$ ns ionization cut.

B. Total $H^{\pm\pm}$ Acceptance

1. Geometric × Kinematic Acceptance

A combination of data and Monte Carlo are used to measure the total acceptance. We measure the geometric times kinematic acceptance of the basic muon and track event selection using the PYTHIA Monte Carlo program [5].

In order to properly simulate a quasi-stable, doubly-charged Higgs, PYTHIA needs to be modified to prevent its immediate decay. We generate massive H^{++}/H^{--} pairs, then immediately change their particle ID, mass, and energy to force them to look like muons when passing through the CDF simulation. In this way, we preserve the doubly-charged Higgs kinematics while allowing for stable particles. We also halve the momentum of each generated particle to account for the detector's assumption of singly-charged particles. Kinematically, the Higgs have a much harder P_T distribution than that of muons from Z. Also, the doubly-charged Higgs events have a much narrower η spectrum compared to their muon counterparts. These two kinematic differences are instrumental in enhancing the geometric times kinematic acceptance of the $Z^0 \to H^{++}H^{--}$ events. This acceptance is shown along with the loose and tight $H^{\pm\pm}$ efficiencies in Figure 1.

2. $H^{\pm\pm}$ ID Efficiency

The efficiency for identifying isolated high P_T muons in the data is measured by selecting $Z \to \mu\mu$ events where one muon is fully identified and the second muon is only a track. We then measure how frequently this track satisfies all muon identification criteria. We square the efficiency for every requirement we make on both particles (muon and track) in an event. The cosmic ray tagger has been shown to be 100% efficient, with an upper limit of 0.8% on the inefficiency. Thus the cosmic tagger efficiency is considered to be $100.0^{+0.0}_{-0.8}$%.

The use of muons for measuring the efficiency of a doubly-charged particle may not give an accurate measurement due to edge effects in muon towers and multiple scattering. The edge effects would potentially affect the efficiency of our cut on the isolation of the particle. Considering only the region of a muon tower within 0.5 cm of the tower's edge being capable of generating these effects (only about 7% of the total tower area), we apply an additional inefficiency of (5 ± 5)% on the $H^{\pm\pm}$ ID efficiency. Multiple scattering was studied for low P_T upsilon tracks, and on the order of 1% reduction in efficiency was observed. Thus it was determined that multiple scattering would have only negligible effect on high P_T, massive, doubly-charged Higgs particles.

Efficiencies were also calculated for the calorimetry highly ionizing cuts. We counted the number of cosmics with ionization values (E_{EM} and E_{Had}) quadrupled that passed each cut. These cosmics represent the doubly-charged signal events and thus they were used in calculating the signal efficiencies.

Since there are limitations in measuring very small pulse widths recorded by COT dE/dx, the lower tail of the quadrupled COT dE/dx variable is cut off. Therefore, it would be incorrect to quote any efficiency by simply counting the number of highly ionizing cosmic events that pass the 35 ns cut. Instead, we collected a high-statistics sample of clean protons in the data. We specifically selected high-ionization protons from this sample in the momentum range of 300 to 350 MeV. We selected this momentum range since the COT dE/dx peak is found at approximately the same value as for the quadrupled cosmic sample representing $H^{\pm\pm}$ ionization. This distribution has a tail, which we use in calculating an efficiency for COT dE/dx.

These measured efficiencies are applied directly in the Monte Carlo. The total detection efficiencies (loose or tight) shown in Figure 1 are the product of the geometric×kinematic acceptance and the $H^{\pm\pm}$ ID efficiency.

III. BACKGROUNDS

One advantage of performing a search for a long-lived doubly-charged particle is the lack of SM background. We expect the background to come in the form of highly ionizing muons, electrons, hadronic taus, and QCD jets. All four of these backgrounds were measured using fake rates from either the data or appropriate Monte Carlo as we describe separately for each type below.

For the muon fake rate measurement we select cosmic rays from data as a pure muon sample. We apply cuts using our three dE/dx variables on the cosmics to identify high ionization tracks. The respective fake rates for the cuts are then measured by observing how many cosmics in the sample pass these high ionization cuts. Since track density is lower in cosmic events than in collider-type events and overlapping tracks can artificially increase ionization, we scaled the fake rate accordingly.

We use $W \to e\nu$ Monte-Carlo events as a sample for the electron fake rate measurement. We look in this electron sample for reconstructed "muons" passing the track fiducial and quality cuts. From this track selection we calculated

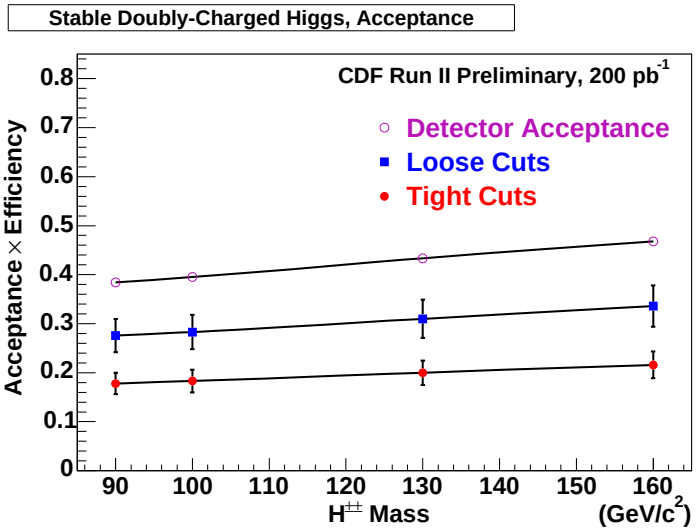

FIG. 1: Product of acceptance and efficiency corresponding to loose and tight ionization cuts. Also shown is the net fiducial and kinematic acceptance at various $H^{\pm\pm}$ masses before efficiencies are included.

the fake rate by counting the fraction which also pass the muon stub cuts and the high ionization cuts. An event of this type would both have to deposit a portion of it's energy in the electromagnetic calorimeter, and also must slip through a crack in the detector and deposit energy in the hadronic calorimeter as well.

A tau decaying hadronically could in theory have high enough ionization in the detector to pass the doubly charged Higgs ionization cuts and also punch through into the muon chamber. Since muon and electron final products are included in our previous two fake rates, we select only hadronic taus from simulation and calculate the fake rate from the number passing the ionization cuts.

Lastly, we consider the case where unbiased jet events are misidentified as highly ionizing particles. We select a base track sample that pass the standard kinematic and quality track cuts, but with the isolation ratio loosened to < 1.0. We then check for highly-ionizing events in this sample by counting the number of tracks which pass both the tightened isolation ratio and the highly ionizing cuts. This misidentified jet background is predicted to be the largest of the categories, so we used a cross-check to confirm its validity. We looked in the high P_T muon data for single track events passing our track, stub, and ionization cuts having $\not\!\!E_T < 20$ GeV. We found 0 such events using both our loose and tight ionization cuts. This absence of low $\not\!\!E_T$ candidate events shows that our QCD fake rate measured from jets is an overestimate. Therefore we use the fake rate from this muon control sample for an improved QCD fake rate. The results of these QCD background calculations, along with the other three backgrounds are shown in Table I.

IV. SYSTEMATIC UNCERTAINTIES

There are several sources of systematic uncertainties in the analysis, and we measure here the relative errors introduced by these uncertainties. We consider the following sources: luminosity, K factor, PDF cross section, PDF acceptance, trigger efficiency, Z_{vtx} efficiency, ID efficiency, cosmic efficiency, energy scale, and energy resolution. Since all these sources of error contribute to the uncertainty applied to our Bayesian analysis, we list them here in one place. We point out though that both the K factor and PDF cross section errors correspond only to the theoretical cross-section and are not included with the others in the net systematic error on the experimental cross section.

The largest systematic errors come from ID efficiency (from the potential ionization edge effects) and errors on the NLO cross section due to NNLO contributions. The ID efficiency uncertainty introduces a systematic error of 12.3%. The theoretical cross sections at next-to-leading-order (NLO) for the doubly charged Higgs contain systematic errors coming from renormalization and factorization scale dependence which were estimated at the time of their calculation to be between $5 - 10\%$ [6]. For our systematic error, we take the central value in the stated range, 7.5%. Other systematics exceeding 1% are the acceptance and cross section uncertainties based on PDF choice (roughly 6% depending on the $H^{\pm\pm}$ mass) and a luminosity uncertainty of 6%. Adding all our systematics in quadrature (except for the correlated PDF uncertainties which we add linearly) gives us a total systematic error of about 16.8%.

V. RESULTS

Upon unblinding to the data, we found 0 loose and 0 tight $H^{\pm\pm}$ candidates. Table I shows a summary of the background estimates for each search topology along with the number of candidates found in the data.

CDF Run II Preliminary, 200 pb^{-1}

Background Source	Loose Search	Tight Search
Z$\rightarrow \mu\mu$	$< 10^{-6}$	$< 10^{-12}$
Z$\rightarrow ee$	$< 10^{-6}$	$< 10^{-7}$
Z$\rightarrow \tau\tau$	$< 10^{-9}$	$< 10^{-9}$
Jet Misidentified	$< 10^{-5}$	$< 10^{-6}$
Total Background	$< 10^{-5}$	$< 10^{-6}$
Data Candidates	0	0

TABLE I: Background summary and number of candidate $H^{\pm\pm}$ events.

We calculate the Bayesian upper limit on the cross section in the usual way:

$$\sigma_{H^{\pm\pm}} = \frac{\text{Upper limit on \# of signal events at 95\% C.L. given 0 events observed}}{A_{H^{\pm\pm}} \times \int \mathcal{L}dt} \tag{2}$$

where $A_{H^{\pm\pm}}$ is the total acceptance (geometrical and kinematic times efficiency) and $\int \mathcal{L}dt$ the integrated luminosity of 206 pb^{-1}.

For a central $H^{\pm\pm}$ mass of 130 GeV/c^2, this equation gives a cross section of $0.0507 \pm 0.0066 \pm 0.0030$ pb where the first uncertainty is statistical and the second is systematic.

Figure 2 shows the theoretical and 95% C.L. cross section limits for our doubly-charged Higgs search. We use the intersection of these two curves to set a mass limit of 134 GeV/c^2 for production of quasi-stable doubly-charged Higgs.

A previous limit for stable $H^{\pm\pm}$ of 97.3 GeV/c^2 was set by the DELPHI collaboration [3]. Therefore, the limit we set here is the best limit for this type of particle.

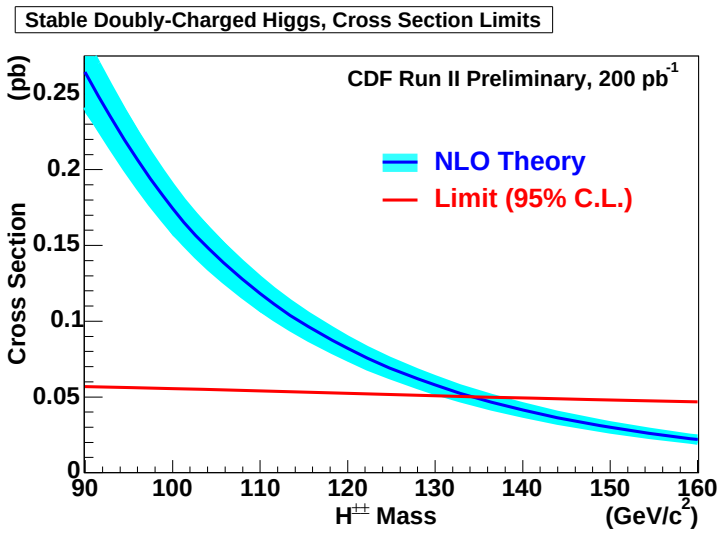

FIG. 2: The theoretical and experimental $H^{\pm\pm}$ cross section limits for the loose ionization cuts. The intersection corresponds to a long-lived doubly-charged Higgs mass limit for the analysis of 134 GeV/c^2.

Acknowledgments

We thank the Fermilab staff and the technical staffs of the participating institutions for their vital contributions. This work was supported by the U.S. Department of Energy and National Science Foundation; the Italian Istituto

Nazionale di Fisica Nucleare; the Ministry of Education, Culture, Sports, Science and Technology of Japan; the Natural Sciences and Engineering Research Council of Canada; the National Science Council of the Republic of China; the Swiss National Science Foundation; the A.P. Sloan Foundation; the Bundesministerium fuer Bildung und Forschung, Germany; the Korean Science and Engineering Foundation and the Korean Research Foundation; the Particle Physics and Astronomy Research Council and the Royal Society, UK; the Russian Foundation for Basic Research; the Comision Interministerial de Ciencia y Tecnologia, Spain; and in part by the European Community's Human Potential Programme under contract HPRN-CT-20002, Probe for New Physics.

[1] F. Abe, et al., Nucl. Instrum. Methods Phys. Res. A **271**, 387 (1988); D. Amidei, et al., Nucl. Instum. Methods Phys. Res. A **350**, 73 (1994); F. Abe, et al., Phys. Rev. D **52**, 4784 (1995); P. Azzi, et al., Nucl. Instrum. Methods Phys. Res. A **360**, 137 (1995); The CDFII Detector Technical Design Report, Fermilab-Pub-96/390-E
[2] CDF II Collaboration, arXiv:hep-ex/0406073.
[3] J. Abdallah, et al., Phys. Lett. B., **552**, 127 (2003).
[4] D. E. Groom, et al., Eur. Phys. J., **C15**, 1 (2000).
[5] T. Sjostrand et al., High-Energy-Physics Event Generation with PYTHIA 6.1, Comput. Phys. Commun. **135**, 238 (2001).
[6] M. Muhlleitner and M. Spira, Phys. Rev. D., **68**, 117701 (2003).